

Phase Transitions in Systems with Aggregation and Shattering

P. L. Krapivsky,¹ W. Otieno,² and N. V. Brilliantov²

¹*Department of Physics, Boston University, Boston, MA 02215, USA*

²*Department of Mathematics, University of Leicester, Leicester LE1 7RH, UK*

We consider a system of clusters made of elementary building blocks, monomers, and evolving via collisions between diffusing monomers and immobile composite clusters. In our model, the cluster-monomer collision can lead to the attachment of the monomer to the cluster (addition process) or to the total break-up of the cluster (shattering process). A phase transition, separating qualitatively different behaviors, occurs when the probability of shattering events exceeds a certain threshold. The novel feature of the phase transition is the dramatic dependence on the initial conditions.

I. INTRODUCTION

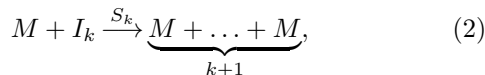
Addition is the basic growth mechanism generating objects of potentially unlimited size. In the simplest implementation the process begins with a vast number of identical elementary building blocks, monomers, and larger objects are formed by adding monomers. The smallest composite objects, dimers, arise via the reaction process $M + M \rightarrow I_2$, where $M = I_1$ denotes a monomer. A trimer is formed by adding a monomer to a dimer, $M + I_2 \rightarrow I_3$, and generally



We tacitly assume that each cluster is fully described by a single parameter, its mass k which is the number of constituent monomers; the addition process (1) is then characterized by the collection of addition rates A_k .

The addition process (1) mimics aggregating systems in which monomers are mobile, while composite objects (clusters) are immovable. In contrast to the classical aggregation kinetics where all clusters react with each other [1–3], clusters do not directly interact in the process (1), they just gradually grow by the addition of monomers. The model (1) has been used to mimic numerous processes, see e.g. [4–10] and references therein. Addition processes also underlie self-assembly, see [11–15]. One important application of this model is to surface science where the monomers are adatoms hopping on the substrate, see e.g. [16–22]. When two adatoms meet they form an *immobile* island, a dimer; similarly when an adatom meets an island I_k , it attaches irreversibly forming an island I_{k+1} of mass $k + 1$.

The opposite processes of clusters decomposition are also possible when a cluster collides with an energetic monomer. In this case the energy of the adatom, transmitted to the island, can break some bonds between adatoms comprising the island. Here we investigate the extreme version positing that clusters undergo a total break-up (shattering) into constituting monomers:



where $k \geq 2$ and S_k are the shattering rates. As we show below, the interplay between addition and shattering generically results in a phase transition. Namely,

with increasing shattering rates the stationary concentrations of clusters undergo a discontinuous jump when shattering rates exceeds some threshold. In particular, if the shattering events are rare the stationary concentration of monomers vanishes, while it becomes finite above the critical shattering rate. This critical rate demarcates qualitatively different states of the system: For the super-critical shattering the system reaches an equilibrium stationary state independent on the initial conditions. For the sub-critical shattering, the stationary states are jammed, that is, they are determined by the initial conditions. Surprisingly, the critical shattering depends on the initial conditions of the system itself.

II. ADDITION AND SHATTERING WITH MASS-INDEPENDENT RATES

We start our analysis with the simplest model in which the addition and shattering rates are mass independent:

$$A_k = 1, \quad S_k = \lambda \quad (3)$$

In the context of surface science, the mass-independent addition rate is particularly natural in the realm of the point-island model (where each island occupies a single lattice site), and in the most interesting case of two-dimensional substrate it provides a good approximation in more realistic cases [16–20].

The evolution equations for the addition-and-shattering model with rates (3) read

$$\frac{dc_1}{dt} = -c_1^2 - c_1 \sum_{j \geq 1} c_j + \lambda c_1 \sum_{j \geq 2} j c_j, \quad (4a)$$

$$\frac{dc_k}{dt} = c_1 c_{k-1} - c_1 c_k - \lambda c_1 c_k, \quad k \geq 2. \quad (4b)$$

Here c_k is the density of clusters of mass k , so $k = 1$ corresponds to mobile adatoms and $k \geq 2$ describe immobile islands. These equations are the straightforward generalization of the addition model [4] where $\lambda = 0$. The first and second terms in the right-hand side of Eq. (4a) give the rate of monomers loss due to aggregation, while the third term quantifies the gain of monomers in the shattering events (2) with $S_k = \lambda$. Similarly, the three terms in the right-hand side of Eq. (4b) describe respectively

the gain of k -mers in the reactions of monomers with the $(k-1)$ -mers and loss of the k -mers in the aggregation and shattering processes.

Using (4a)–(4b) one can verify that the mass density $\sum_{j \geq 1} j c_j$ remains constant throughout the evolution. We shall set the mass density to unity if not stated otherwise

$$M = \sum_{j \geq 1} j c_j = 1 \quad (5)$$

if not stated otherwise. This can be done without loss of generality. Indeed, the right-hand side of the rate equations (4a)–(4b) are quadratic polynomials and hence the rate equations are invariant under the transformation $t \rightarrow t/M$ and $c_k \rightarrow M c_k$. With this transformation one can always set the mass density to unity.

Introducing the auxiliary time

$$\tau = \int_0^t dt' c_1(t') \quad (6)$$

we linearize the above equations

$$\frac{dc_1}{d\tau} = \lambda - (1 + \lambda)c_1 - N, \quad N = \sum_{j \geq 1} c_j \quad (7a)$$

$$\frac{dc_k}{d\tau} = c_{k-1} - (1 + \lambda)c_k, \quad k \geq 2 \quad (7b)$$

$$\frac{dN}{d\tau} = \lambda - (1 + \lambda)N. \quad (7c)$$

We used the relation $\sum_{j \geq 2} j c_j = 1 - c_1$ which follows from (5) and displayed the rate equation for the total cluster density, $N(\tau)$, obtained by summing (7a) and Eqs. (7b) for all $k \geq 2$.

We shall always use the mono-disperse initial condition

$$c_k(0) = \delta_{k,1} \quad (8)$$

if not stated otherwise. Solving (7c) subject to $N(0) = 1$ gives

$$N = \frac{\lambda + e^{-(1+\lambda)\tau}}{1 + \lambda}. \quad (9)$$

Plugging (9) into (7a) we obtain a close equation for the density of monomers which is solved to yield

$$c_1 = \left[1 - \frac{\tau}{1+\lambda}\right] e^{-(1+\lambda)\tau} + \frac{\lambda^2}{(1+\lambda)^2} \left[1 - e^{-(1+\lambda)\tau}\right]. \quad (10)$$

To find the evolution of the island densities, we apply to Eqs. (7b) the Laplace transform, $\hat{c}_k = \int_0^\infty c_k(\tau) e^{-p\tau} d\tau$. Since $c_k(0) = 0$ for $k \geq 2$, we obtain

$$p\hat{c}_k = \hat{c}_{k-1} - (1 + \lambda)\hat{c}_k, \quad k \geq 2, \quad (11)$$

from which

$$\hat{c}_k(p) = \frac{\hat{c}_1(p)}{(p + 1 + \lambda)^{k-1}}, \quad k \geq 2. \quad (12)$$

It is straightforward to find the Laplace transform of $c_1(\tau)$ given by (10); substituting the result into Eq. (12) and performing the inverse Laplace transform we obtain

$$c_{k+1}(\tau) = \frac{\tau^k}{\Lambda k!} \left[\frac{2\Lambda - 1}{\Lambda} - \frac{\tau}{k+1} \right] e^{-\Lambda\tau} + \frac{(\Lambda - 1)^2 \gamma(k, \Lambda\tau)}{\Lambda^{k+2} (k-1)!} \quad (13)$$

where

$$\gamma(k, a) = \int_0^a du u^{k-1} e^{-u} \quad (14)$$

is the incomplete Gamma function. Hereinafter we often use the shorthand notation $\Lambda \equiv \lambda + 1$. If we assume that $\tau \rightarrow \infty$ as $t \rightarrow \infty$, Eqs. (9) and (13) give the asymptotic distribution for clusters size and total cluster density:

$$C_k \equiv c_k(\tau = \infty) = \frac{\lambda^2}{(1 + \lambda)^{k+1}} \quad k \geq 1, \quad (15)$$

$$N(\tau = \infty) = \frac{\lambda}{1 + \lambda}. \quad (16)$$

Exactly the same result is obtained if one seeks the stationary solution to Eqs. (7a)–(7c).

Naively, one would expect that the system evolves to the equilibrium state (15)–(16) independently on initial conditions. Yet the system demonstrates a richer behavior, see Fig. 1. As one can see from Fig. 1, the densities may relax to a state dramatically different from the equilibrium solution (15)–(16).

To understand this surprising behavior we notice that the monomer density given by (10) is physically applicable as long as $c_1 \geq 0$. For sufficiently large shattering rates the monomer density is always positive, while for smaller rates $c_1(\tau)$ first vanishes at a certain $\tau_{\max}(\lambda)$. In these situations, the physical range $0 \leq t < \infty$ corresponds to $0 \leq \tau < \tau_{\max}(\lambda)$, so that the above assumption, that $t \rightarrow \infty$ as $\tau \rightarrow \infty$ is not valid. More precisely, $\tau_{\max}(\lambda)$ is finite when $\lambda \leq \lambda_c$, while for $\lambda > \lambda_c$ the monomer density remains positive for all $0 < \tau < \infty$. This is obvious from Fig. 2. To establish this assertion analytically we first notice that $c_1(\tau)$ given by (10) reaches minimum when $\tau = 2$, from which the minimal possible value is

$$c_1^{\min} = \left[1 - \frac{2}{1 + \lambda}\right] e^{-2(1+\lambda)} + \frac{\lambda^2}{(1 + \lambda)^2} \left[1 - e^{-2(1+\lambda)}\right].$$

Analyzing this expression we find that it remains positive when $\lambda > \lambda_c$ where λ_c is the root of $e^{1+\lambda_c} = 1/\lambda_c$, that is, $\lambda_c = W(1/e)$, where $W(x)$ is the Lambert function; numerically $\lambda_c = 0.27846\dots$

Different behaviors emerge depending on whether λ is smaller, equal, or larger than λ_c .

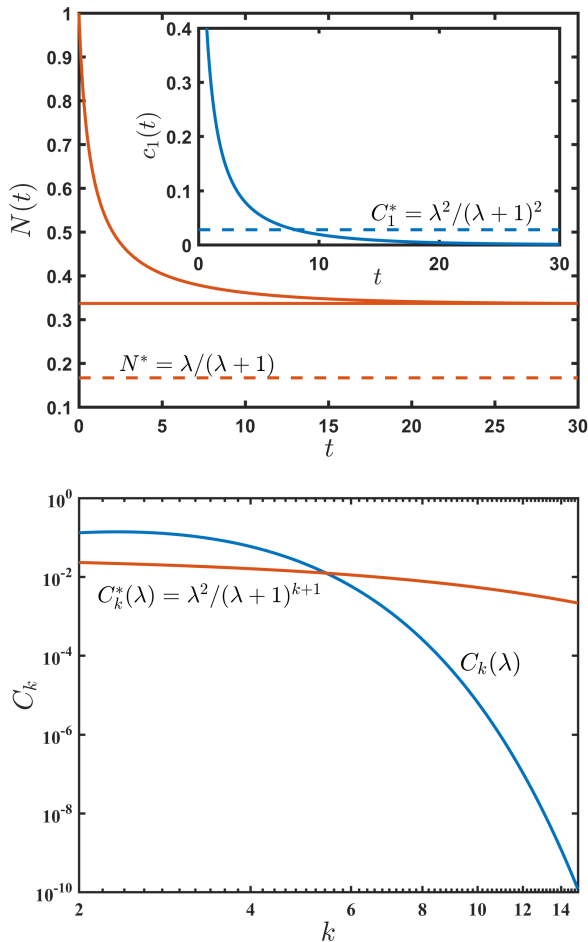


FIG. 1: Top: Evolution of the monomer density $c_1(t)$ and total cluster density $N(t)$ for the case of constant kernels and the mono-disperse initial condition when $\lambda = 0.2$. The system approaches a final state $c_1(t = \infty)$ and $N(t = \infty)$ which differs from the equilibrium state (15)–(16). Bottom: Asymptotic cluster size distribution, $c_k(t = \infty)$, dramatically differs from the equilibrium distribution (15).

A. Sub-critical regime: $\lambda < \lambda_c$

In the region $0 \leq \lambda < \lambda_c$ the monomer density vanishes at a certain $\tau_{\max}(\lambda)$ which is found from (10) to be the root of the transcendental equation

$$e^{(1+\lambda)\tau_{\max}} = \frac{(1+\lambda)\tau_{\max} - 1 - 2\lambda}{\lambda^2} \quad (17)$$

The solution of Eq. (17) may be expressed in terms of the Lambert function:

$$\tau_{\max} = \frac{1 + 2\lambda - W(-\lambda^2 e^{2\lambda+1})}{1 + \lambda} \quad (18)$$

Note that τ_{\max} increases from 1 to 2 as λ increases from 0 to λ_c , see Fig. 2. For $\tau_{\max} = 1$ and $\lambda = 0$, Eq. (13) reproduces the final distribution of cluster sizes for the additional aggregation without shattering [4].

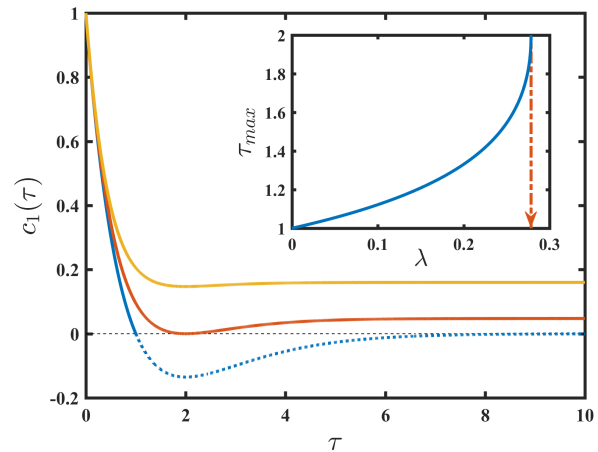


FIG. 2: The monomer density $c_1(\tau)$ remains positive when the shattering rate satisfies $\lambda > \lambda_c \approx 0.27846$. Shown (bottom to top) is the monomer density for $\lambda = 0, \lambda_c, 2/3$. Inset: When physical time diverges, $t \rightarrow \infty$, the auxiliary time for $\lambda < \lambda_c$, remains finite, $\tau \rightarrow \tau_{\max}(\lambda)$.

The monomer density vanishes exponentially in terms of the physical time,

$$c_1 \sim e^{-t(N_\infty - \lambda)} \quad t \rightarrow \infty,$$

and the island densities saturate at $t \rightarrow \infty$, that is, $C_k(\lambda) \equiv c_k(\tau_{\max}) > 0$ for $k \geq 2$, with $c_k(\tau)$ and τ_{\max} given respectively by Eqs. (13) and (18); the same is true for the final density of islands $N_\infty(\lambda) = N[\tau_{\max}(\lambda)]$ which is positive for all $\lambda \geq 0$.

Analyzing (9) and (17) one finds that in the subcritical region $N_\infty(\lambda)$ is a decreasing function of the shattering rate λ , namely it decreases from $N_\infty(0) = e^{-1} \approx 0.36788$ to $N_\infty(\lambda_c) = \lambda_c$, see Fig. 3. The approach of $N_\infty(\lambda)$ to the density $N_\infty(\lambda_c) = \lambda_c$ in the critical regime is singular:

$$N_\infty(\lambda) - N_\infty(\lambda_c) \simeq 2\lambda_c \sqrt{\frac{\lambda_c}{1 + \lambda_c}} \sqrt{\lambda_c - \lambda} \quad (19)$$

as $\lambda \uparrow \lambda_c$.

B. Critical regime: $\lambda = \lambda_c$

In the critical regime the monomer density (10) also vanishes. More precisely, when $\tau \rightarrow \tau_{\max}(\lambda_c) = 2$, the monomer density decreases as $c_1 \simeq \frac{1}{2}\lambda_c^2(2 - \tau)^2$ which can be re-written as

$$c_1(t) \simeq \frac{2}{\lambda_c^2} \frac{1}{t^2} \quad (20)$$

in terms of the original time variable. Thus in the critical regime the process slows down — the vanishing is algebraic rather than exponential.

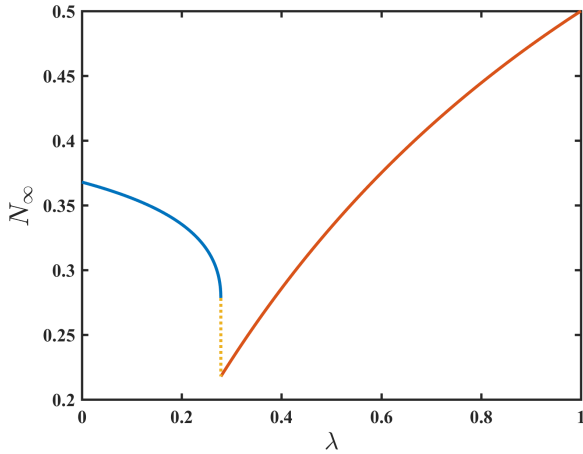


FIG. 3: The final density of clusters $N_\infty(\lambda)$ is a decreasing function of λ in the range $0 \leq \lambda \leq \lambda_c \approx 0.27846$, it undergoes a first order transition at λ_c , and becomes an increasing function of λ in the range $\lambda > \lambda_c$ where $N_\infty = N^* = \lambda/(1 + \lambda)$.

The total density of clusters also exhibits an algebraic approach to the final density:

$$N(t) - N_\infty \simeq \frac{2}{t} \quad (21)$$

where $N_\infty = N_\infty(\lambda_c) = \lambda_c$. The asymptotic (21) follows from (9). The decay exponent in (21) is twice smaller than the exponent characterizing the decay of monomers.

The approach to the final density for any species of islands is similar to (21), viz.

$$c_k(t) - C_k \simeq \frac{B_k}{t}. \quad (22)$$

Using (4b) one can express the amplitudes B_k through the final densities $C_k \equiv c_k(\tau = 2)$:

$$B_k = 2 \frac{\Lambda_c C_k - C_{k-1}}{(\Lambda_c - 1)^2}, \quad \Lambda_c = 1 + \lambda_c \quad (23)$$

for $k \geq 2$. The final densities can be expressed using Eq. (13) with $\tau_{\max} = 2$. One finds

$$\begin{aligned} \frac{C_{k+1}}{(\Lambda_c - 1)^2} &= \frac{2^k}{\Lambda_c k!} \left[\frac{2\Lambda_c - 1}{\Lambda_c} - \frac{2}{k+1} \right] \\ &+ \frac{\gamma(k, 2\Lambda_c)}{\Lambda_c^{k+2} (k-1)!} \end{aligned} \quad (24)$$

Combining (24) with (23) we get

$$B_k = -2^{k-1} \frac{(k-1)(k-4)}{k!} \quad (25)$$

where we have used the identity

$$(k-1)\gamma(k-1, 2\Lambda) - \gamma(k, 2\Lambda) = (2\Lambda)^{k-1} e^{-2\Lambda} \quad (26)$$

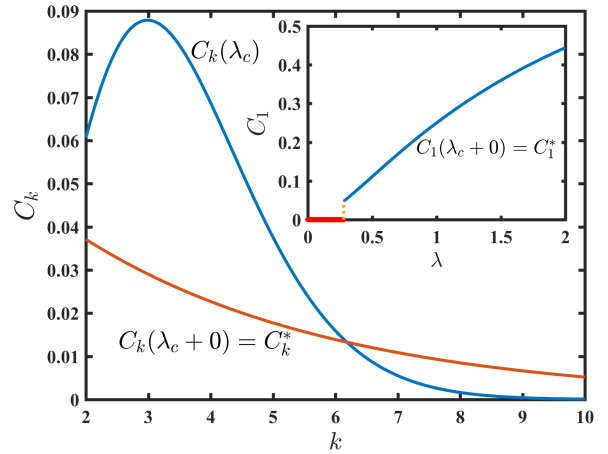


FIG. 4: The discontinuous jump in the cluster size distribution from $C_k(\lambda_c)$ to $C_k(\lambda_c + 0)$, given by Eq. (15) at the critical point $\lambda = \lambda_c$. Inset: The final density of monomers $C_1(\lambda)$ vanishes in the range $0 \leq \lambda \leq \lambda_c \approx 0.278465$, undergoes a first order transition at λ_c , and becomes an increasing function of λ in the super-critical region $\lambda > \lambda_c$ where $C_1 = \lambda^2/(1 + \lambda)^2$.

which can be derived by substituting the definition (14) into (26) and performing the integration by part of the second integral on the left-hand side. We also use the identity $e^{-\Lambda_c} = \Lambda_c - 1$ obeyed by $\Lambda_c = 1 + \lambda_c$. Remarkably, the amplitudes B_k are independent on Λ_c and rational.

C. Super-critical region: $\lambda > \lambda_c$

In the super-critical case $\tau \rightarrow \infty$ as $t \rightarrow \infty$ and we can use Eq. (15) for the final cluster densities $C_k(\lambda)$:

$$C_k(\lambda) = \frac{\lambda^2}{(1 + \lambda)^{k+1}} = C_k^* \quad k \geq 1. \quad (27)$$

Thus the final monomer density exhibits a discontinuous (first order) phase transition as a function of λ :

$$C_1(\lambda) = \begin{cases} 0 & \lambda \leq \lambda_c \\ \frac{\lambda^2}{(1+\lambda)^2} & \lambda > \lambda_c \end{cases} \quad (28)$$

see Fig. 4. The total cluster density also exhibits the discontinuous phase transition at $\lambda = \lambda_c$, more precisely

$$N_\infty(\lambda) = \begin{cases} \lambda_c & \lambda = \lambda_c \\ \frac{\lambda_c}{1+\lambda_c} & \lambda = \lambda_c + 0 \end{cases} \quad (29)$$

The same is valid for the final densities C_k which undergo a jump at the critical point $\lambda = \lambda_c$ from the values $C_k(\lambda_c)$, given by Eq. (24), to $C_k(\lambda_c + 0) = \lambda_c^2/(1 + \lambda_c)^{k+1}$, as it illustrated in Fig. 4.

D. Dependence on initial conditions

The previous analysis has been done for the mono-disperse initial condition (8). We now briefly discuss more general initial conditions. (We still set $M = 1$.)

The behavior in the super-critical region is universal, e.g. the final densities are given by (27) do not depend on the initial condition. The critical shattering rate is not universal, however, namely it depends on the initial condition. As an example, consider the initial condition

$$c_1(0) = c_2(0) = 1/3, \quad c_k(0) = 0 \quad \text{when } k \geq 3, \quad (30)$$

which corresponds to $N(0) = 2/3$. Performing the same steps that led to Eq. (10), we obtain the monomer density for the above initial conditions:

$$c_1 = \frac{1}{3} \left[1 - \frac{2-\lambda}{1+\lambda} \tau \right] e^{-(1+\lambda)\tau} + \frac{\lambda^2}{(1+\lambda)^2} \left[1 - e^{-(1+\lambda)\tau} \right].$$

The qualitative behaviors remain the same. Chief quantitative results are also universal, e.g., in the critical regime the monomer density exhibits the t^{-2} decay. The critical shattering rate is however $\lambda_c \approx 0.30057$ for the initial condition (30).

For an arbitrary initial conditions solution of Eqs. (7a), (7c) yield for the total cluster and monomer density

$$N(\tau) = \frac{\lambda}{1+\lambda} \left[1 - e^{-(1+\lambda)\tau} \right] + N_0 e^{-(1+\lambda)\tau}, \quad (31)$$

$$c_1(\tau) = c_{1,0} e^{-(1+\lambda)\tau} - \left[N_0 - \frac{\lambda}{1+\lambda} \right] \tau e^{-(1+\lambda)\tau} + \frac{\lambda^2}{(1+\lambda)^2} \left[1 - e^{-(1+\lambda)\tau} \right], \quad (32)$$

where $N_0 = N(0)$ and $c_{1,0} = c_1(0)$. Preforming again the Laplace transform and using the Laplace transform of $c_1(\tau)$ given by (32), we find the clusters size distribution for arbitrary initial conditions:

$$c_{k+1}(\tau) = \frac{\tau^k}{k!} \left[c_{1,0} - C_1^* - (N_0 - N^*) \frac{\tau}{k+1} \right] e^{-\Lambda\tau} + \frac{(\Lambda - 1)^2 \gamma(k, \Lambda\tau)}{\Lambda^{k+2} (k-1)!} + c_{k,0} e^{-\Lambda\tau} \quad (33)$$

Here $c_{k,0} = c_k(0)$ and we use the shorthand notations $N^* \equiv \lambda/(1+\lambda)$ for the equilibrium cluster density and $C_1^* \equiv \lambda^2/(1+\lambda)^2$ for the equilibrium density of monomers.

There are again three regimes. In the super-critical regime, $c_1(\tau) > 0$ for all τ . In this case $\tau \rightarrow \infty$ as $t \rightarrow \infty$ and the final distribution (27) of cluster sizes C_k is universal and independent on the initial conditions. In the sub-critical regime, $c_1(\tau) \geq 0$ for $\tau \leq \tau_{\max}$ and $c_1(\tau) < 0$ otherwise. In the critical regime, $c_1(\tau) \geq 0$ for all τ , and $c_1(\tau_{\max}) = 0$. For the critical and sub-critical regimes, $\tau \rightarrow \tau_{\max} < \infty$ as $t \rightarrow \infty$ and the distribution C_k is not universal, namely it depends on the initial conditions.

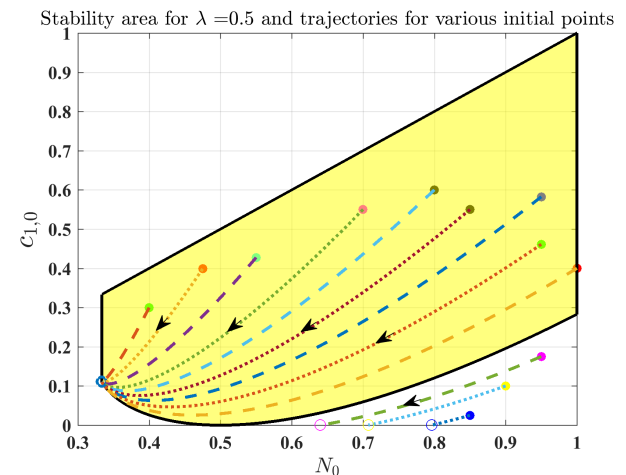
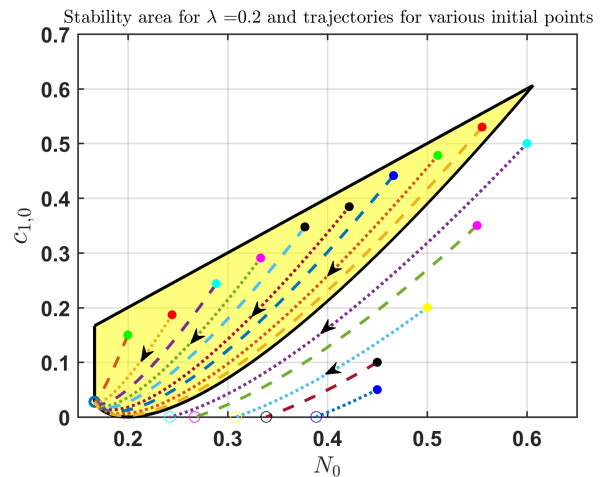


FIG. 5: Phase trajectories for the total density $N(t)$ and the density of monomers $c_1(t)$ for different initial conditions. The region marked by yellow corresponds to the super-critical regime, where all trajectories terminate at the universal point, $N^* = \lambda/(1+\lambda)$, $C_1^* = \lambda^2/(1+\lambda)^2$. The curved part of this boundary of the yellow domain corresponds to the critical regime. For the initial conditions, located outside the yellow domain (and satisfying $c_{1,0} \leq N_0$) the sub-critical regime is realized; the trajectories terminate in this case on the axis $c_1 = 0$.

We emphasize that two parameters, N_0 and $c_{1,0}$, play the crucial role in the critical and sub-critical regimes as they demarcate the emergence of these regimes and determine the final modified time τ_{\max} . Using (32) one can find the domain in the $(N_0, c_{1,0})$ phase plane where $c_1(\tau) > 0$ for all τ [23]

$$\frac{(1+\lambda)c_{1,0} + N_0 - \lambda}{N_0 - N^*} > \ln \left(\frac{N_0 - N^*}{\lambda N^*} \right). \quad (34)$$

(Needless to say, $c_{1,0} \leq N_0$ should be also obeyed). Within this domain, all trajectories in the (N, c_1) plane terminate at the universal point (N^*, C_1^*) . If Eq. (34) turns into equality, it determines the critical shattering

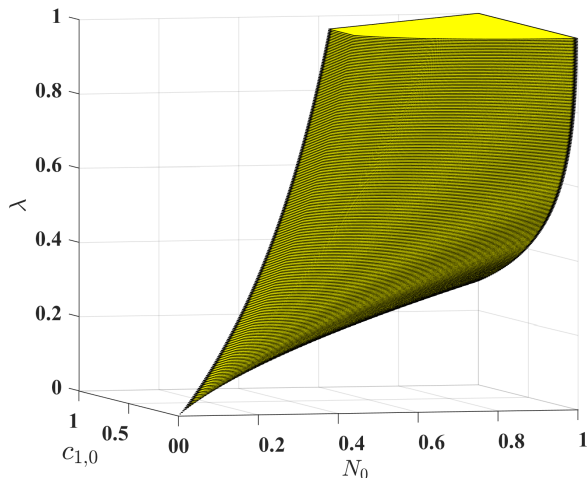


FIG. 6: The 3D plot of the critical shattering λ_c as the function of the initial conditions N_0 , $c_{1,0}$ for the model with constant kinetic rates (3). The domain inside the depicted surface corresponds to the super-critical behavior of the system; Fig. 5 provides the cross-sections of this surface for particular values of λ .

rate λ_c thereby yielding the dependence on the initial conditions: $\lambda_c = \lambda_c(N_0, c_{1,0})$.

Outside of the domain given by (34) the trajectories terminate on the axis $c_1 = 0$ with N_∞ depending on the initial conditions. This is illustrated in Fig. 5.

Figure 6 shows the dependence of the critical shattering λ_c on the initial conditions N_0 and $c_{1,0}$. As it may be seen from the Fig. 6, the larger λ_c the larger the domain of the initial conditions corresponding to the super-critical regime, where the system eventually arrives at the universal steady-state.

III. ADDITION AND SHATTERING WITH ARBITRARY RATES

In the previous section we studied the addition and shattering processes with mass-independent rates (3). A more general class of models is characterized by rates which vary algebraically: $A_k = k^a$ and $S_k = \lambda k^s$. In this section we limit ourselves for the case of $a = s$. We start with $a = s = 1$, which admits some analytical treatment.

A. Kinetic rates proportional to the cluster mass

For the linear dependence of the kinetic rates on the cluster mass, $A_k = k$ and $S_k = \lambda k$, the kinetic equations read

$$\frac{dc_1}{d\tau} = -(1 + \lambda)c_1 - 1 + \lambda M_2 \quad (35a)$$

$$\frac{dc_k}{d\tau} = (k - 1)c_{k-1} - (1 + \lambda)kc_k, \quad k \geq 2 \quad (35b)$$

The second moment $M_2 = \sum_{k \geq 1} k^2 c_k$ of the cluster size distribution appears in (35a). Generally the α^{th} moment is defined by

$$M_\alpha = \sum_{i=1}^{\infty} k^\alpha c_k \quad (36)$$

To determine the monomer density one needs to know M_2 . The rate equation for the second moment is simple,

$$\frac{dM_2}{d\tau} = 2M_2 + \lambda(M_2 - M_3), \quad (37)$$

yet it involves the third moment. The rate equation for the third moment similarly involves the fourth moment. This continues ad infinitum leading to (seemingly) unsolvable hierarchy.

1. Super-critical regime

For the super-critical region $\lambda > \lambda_c$ we easily find the equilibrium densities. Indeed, Eq. (35b) turns into the simple recurrence $(1 + \lambda)kC_k = (k - 1)C_{k-1}$ admitting an exact solution giving the equilibrium cluster size distribution

$$C_k = \frac{C_1}{k(1 + \lambda)^{k-1}}$$

Using the condition for the mass density, $\sum_{k \geq 1} kC_k = 1$, we fix $C_1 = \lambda/(1 + \lambda)$, which yields

$$C_k = \frac{\lambda}{(1 + \lambda)^k} \frac{1}{k} = C_k^* \quad (38)$$

2. Sub-critical and critical regime

First we consider the mono-disperse initial condition. Applying again the Laplace transform to (35b) yields

$$p\hat{c}_k = (k - 1)\hat{c}_{k-1} - (1 + \lambda)k\hat{c}_k, \quad k \geq 2 \quad (39)$$

Solving this recurrence we express all $\hat{c}_k(p)$ through $\hat{c}_1(p)$:

$$\hat{c}_k(p) = \frac{\hat{c}_1(p)}{(1 + \lambda)^{k-1}} \frac{\Gamma(k)\Gamma(1 + \Pi)}{\Gamma(k + \Pi)} \quad (40)$$

with $\Pi = 1 + (1 + \lambda)^{-1}p$. Applying the Laplace transform for the mass conservation (5) we obtain

$$\sum_{k \geq 1} k\hat{c}_k(p) = \frac{1}{p}. \quad (41)$$

Plugging then (40) into (41) we find the Laplace transform of the monomer density:

$$\hat{c}_1 = p^{-1} \frac{1}{F[1, 2; 1 + \Pi; (1 + \lambda)^{-1}]} \quad (42)$$

where $F[a, b; c; z] = \sum_{n \geq 0} \frac{(a)_n (b)_n}{(c)_n} \frac{z^n}{n!}$ is the hypergeometric function.

Near the origin, $p \rightarrow 0$ [24], we have $\Pi \rightarrow 2$, and using identity $F[1, 2; 2; z] = (1 - z)^{-1}$, we find that \hat{c}_1 has a simple pole with residue $\lambda/(1 + \lambda)$. This is consistent with the monomer density $c_1(\tau)$ quickly approaching the steady-state value $C_1 = \lambda/(1 + \lambda)$ which agrees with (38).

The precise value of the critical shattering amplitude λ_c corresponding to the mono-disperse initial condition is hidden in the exact Laplace transform of the monomer density (42), but difficult to extract. We now show that $\lambda_c > 0$ at least for some initial conditions.

Let us consider a simple case when initially only monomers and dimers present in the system, so that

$$c_{1,0} = 2N_0 - 1; \quad c_{2,0} = 1 - N_0; \quad M_2(0) = 3 - 2N_0. \quad (43)$$

Equation (35a) becomes

$$\frac{dc_1}{d\tau} = -(1 + \lambda)c_1 - 1 + \lambda(3 - 2N_0)$$

when $\tau \ll 1$. Let almost all clusters are dimers, then starting with $c_{1,0} = 2N_0 - 1 \ll 1$, the monomer density quickly crosses zero if

$$\lambda(3 - 2N_0) < 1 + (1 + \lambda)(2N_0 - 1)$$

that is, $\lambda < N_0/2(1 - N_0)$. Since $N_0 = c_{1,0} + c_{2,0} \simeq c_{2,0}$ and $M = 1 = c_{1,0} + 2c_{2,0} \simeq 2c_{2,0}$, we conclude that $\lambda_c \rightarrow \frac{1}{2}$. Thus in this case (see also Fig. 7)

$$C_1 = \begin{cases} 0 & \lambda < \frac{1}{2} \\ \frac{\lambda}{1 + \lambda} & \lambda > \frac{1}{2}. \end{cases} \quad (44)$$

For the mono-disperse initial conditions the critical value of λ may be found numerically, $\lambda_c = 0.16773277 \dots$. The final concentrations of clusters $C_k(\lambda_c)$, and monomers $C_1(\lambda_c)$, also found numerically, undergo a first-order phase transition to the values $C_k(\lambda_c + 0)$, and monomers $C_1(\lambda_c + 0)$, given by Eq. (38), see Fig. 8.

The dependence of the evolution regime on the initial conditions is not anymore simple, as in the case of constant kernels, when only the concentration of monomers and the total number of clusters were important. For $A_k = k$ and $S_k = \lambda k$ all initial concentrations $c_k(0)$ are determinative. Fig. 9 shows the domain in the space of the initial concentrations of the monomers, $c_{1,0}$, dimers $c_{2,0}$ and trimers, $c_{3,0}$, corresponding to the supercritical regime, when $c_{4,0} = (1 - c_{1,0} - 2c_{2,0} - 3c_{3,0})/4$ and all other initial concentrations are zero, $c_k(0) = 0$ for $k \geq 5$.

B. Kinetic rates $A_k = k^s$ and $S_k = \lambda k^s$.

Here we consider a family of models with rates $A_k = k^s$ and $S_k = \lambda k^s$. We assume that exponent does not exceed unity, $s \leq 1$. This is physically motivated (the rates cannot increase faster than mass) and the models with $s > 1$

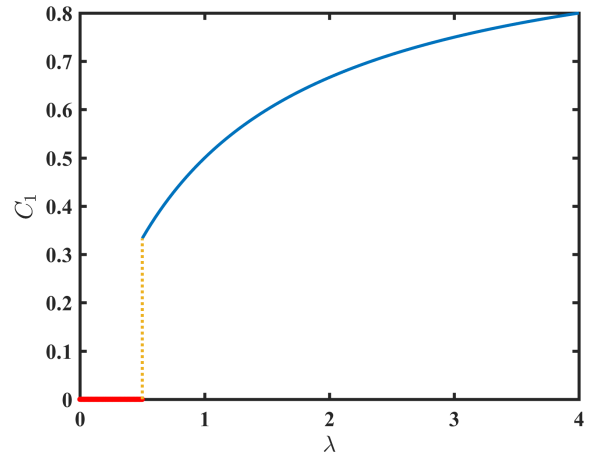


FIG. 7: For the case of linear kernels, $A_k = k$ and $S_k = \lambda k$, the final density of monomers undergoes a first order phase transition at $\lambda = \lambda_c = \frac{1}{2}$. The situation when initially almost all clusters are dimers is shown. The final density of monomers is given by (44) in this case.

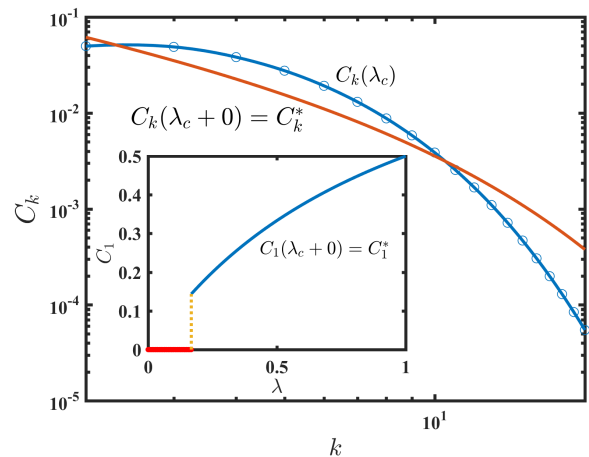


FIG. 8: For the case of linear kernels, $A_k = k$ and $S_k = \lambda k$, the discontinuous jump in the cluster size distribution from $C_k(\lambda_c)$ to $C_k(\lambda_c + 0)$ [see Eq. (38)] happens for mono-disperse initial conditions at the critical point $\lambda_c = 0.16773277 \dots$. Inset: The final density of monomers $C_1(\lambda)$ vanishes in the range $0 \leq \lambda \leq \lambda_c$ and undergoes a first order transition at λ_c . In the super-critical region $\lambda > \lambda_c$, C_1 is given by Eq. (38).

are mathematically ill-defined as instantaneous gelation may occur (it certainly occurs for the pure addition process, see [4, 8]).

The rate equations read

$$\frac{dc_1}{d\tau} = -(1 + \lambda)c_1 - M_s + \lambda M_{1+s} \quad (45a)$$

$$\frac{dc_k}{d\tau} = (k - 1)^s c_{k-1} - (1 + \lambda)k^s c_k, \quad k \geq 2. \quad (45b)$$

These equations involve the moments M_s and M_{1+s} that

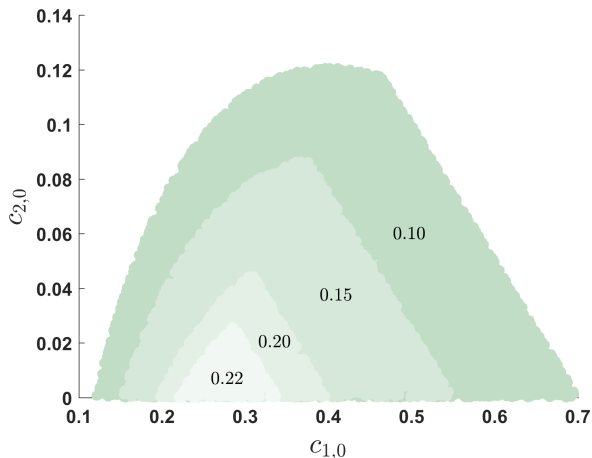


FIG. 9: The boundaries of the super-critical region in the phase plane $(c_{1,0}, c_{2,0})$ for different values of $c_{3,0}$. For each contour, with the value of $c_{3,0}$ indicated on the plot, the super-critical region lies inside the contour. The initial densities $c_{k,0} = 0$ for $k \geq 5$ and $c_{4,0} = (1 - c_{1,0} - 2c_{2,0} - 3c_{3,0})/4$ have been chosen. The rate kernels are $A_k = k$, $S_k = \lambda k$ and $\lambda = 0.16773277\dots$ (which corresponds to λ_c for the mono-disperse initial condition).

satisfy

$$\frac{dM_b}{d\tau} = \sum_{k=1}^{\infty} [(k+1)^b - (1+\lambda)k^b] k^s c_k - M_s + \lambda M_{1+s}$$

with $b = s$ and $b = 1 + s$. These equations are not closed and for non-integer s they cannot be even written in terms of the moments only.

Equations (45a)–(45b) still admit some analytical treatment in the super-critical regime ($\lambda > \lambda_c$). The equilibrium densities straightforwardly follow from the recursion $k^s(1+\lambda)C_k = (k-1)^s C_{k-1}$ and the mass density $M = 1$. One gets

$$C_k = \frac{1}{k^s \Lambda^k \text{Li}_{s-1}(\Lambda^{-1})} \quad (46)$$

where $\Lambda = 1 + \lambda$ as before, and $\text{Li}_\nu(x) = \sum_{j \geq 1} x^j / j^\nu$ is the polylogarithm function. We have $\text{Li}_0(x) = x/(1-x)$ and thus for $s = 1$ we recover the previous result (38).

Overall, our simulations show the same qualitative behavior as for $s = 0$ and $s = 1$. Namely, for any initial condition there exists a supercritical domain with the final densities given by Eq. (46) and $C_1 > 0$. This is illustrated in Fig. 10, where the evolution of monomer density is shown for $s = 0.5$ for supercritical, critical and sub-critical regimes for the case of mono-disperse initial conditions.

The critical shattering rate decreases with increasing s , see Fig. 11, on the interval $0 \leq s \leq 1$. The maximum and minimum values of λ_c are respectively $W(1/e) = 0.2784645\dots$ for $s = 0$ and $0.1677328\dots$ for $s = 1$.

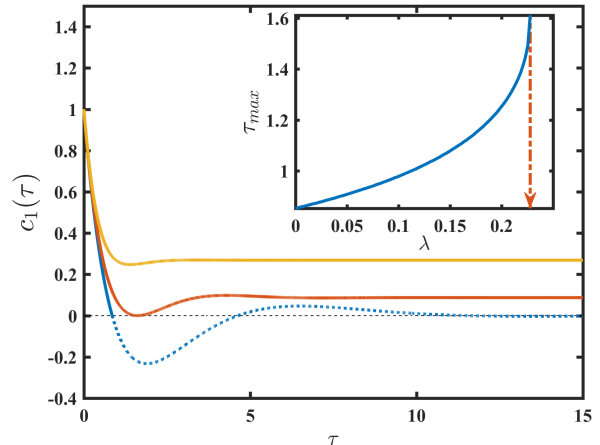


FIG. 10: Evolution of the monomer density $c_1(\tau)$ for super-critical, critical and sub-critical regimes for the mono-disperse initial condition. Shown are results for the model with kernels $A_k = \sqrt{k}$ and $S_k = \lambda\sqrt{k}$. The critical shattering rate in this case is $\lambda_c = 0.2277920103\dots$

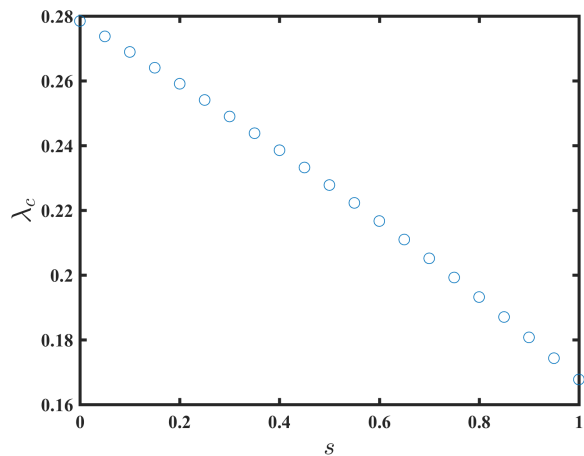


FIG. 11: The dependence of the critical shattering rate λ_c on the exponent s in the case of the mono-disperse initial condition. The critical rate λ_c separates the super-critical evolution regime ($\lambda > \lambda_c$) and sub-critical regime ($\lambda < \lambda_c$).

As in the models with $s = 0$ and $s = 1$, the final densities of clusters C_k and monomers C_1 undergo a jump at the critical point from $C_k(\lambda_c)$ to the super-critical values $C_k(\lambda_c + 0)$ given by (46). As previously, the final monomer density vanishes for the sub-critical and critical case, i.e. $C_1 = 0$ for $\lambda \leq \lambda_c$. The plots for any $0 < s < 1$ look very similar to Figs. 4 and 8.

The dependence of the critical shattering on the initial conditions is again not simple, since λ_c depends on all initial concentrations $c_k(0)$, $k \geq 1$. Accordingly, the super-critical domain depends for each $\lambda > 0$ on all initial concentrations. This is illustrated in Fig. 12, where the boundaries of the super-critical domain are shown.

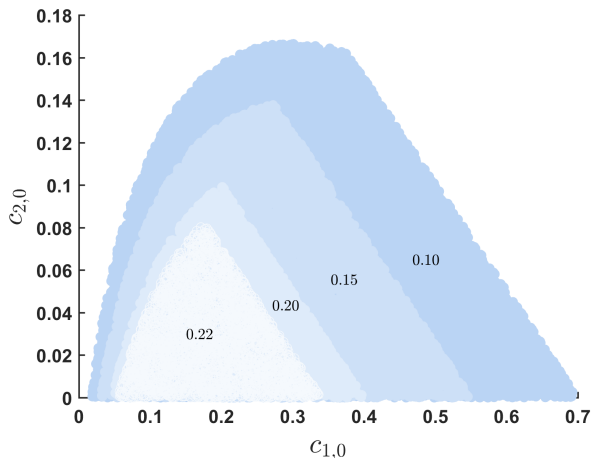


FIG. 12: The boundaries of the super-critical region in the phase plane $(c_{1,0}, c_{2,0})$ for different values of $c_{3,0}$. Shown are results for the model with kernels $A_k = \sqrt{k}$ and $S_k = \lambda\sqrt{k}$ in the case when the initial densities are $c_{k,0} = 0$ for $k \geq 5$ and $c_{4,0} = (1 - c_{1,0} - 2c_{2,0} - 3c_{3,0})/4$. The shattering rate is $\lambda = 0.2277920103\dots$ (it corresponds to λ_c for the mono-disperse initial condition).

IV. CONCLUSION

We investigated a model involving aggregation and fragmentation kinetics where immobile clusters (islands) interact with mobile monomers. The outcome of the monomer-cluster interactions may be twofold—the monomer may attach to the cluster, or the cluster may shatter into monomers. This model mimics the growth of islands on a surface in epitaxy processes when a collision of an adatom (monomer) with an island is accompanied by the transmission of the adatom’s energy to the island. If the transmitted energy is small, the adatom joins the island; if the energy is large, the island may fragment into adatoms. We considered a model when the aggregation rate of a monomer and a cluster of size k depends on k algebraically: $A_k = k^s$. We assumed that the shattering rate at monomer-cluster collisions is proportional to the addition rate, $S_k = \lambda A_k$, where λ quantifies the shattering intensity.

In the model with $s = 0$ the aggregation and shattering rate do not depend on the island size, $A_k = 1$ and $S_k = \lambda$, so the parameter λ characterizes the ratio of shattering and aggregative impacts. This model admits a

comprehensive analytical analysis and demonstrates the most prominent features of aggregating and shattering systems. We also analyzed the model with $s = 1$, and studied numerically the models with $0 < s < 1$. All these models are characterized by three different evolution regimes. In the super-critical regime, $\lambda > \lambda_c$, the system evolves to a final equilibrium state which is universal, i.e., it does not depend on the initial conditions. For the critical and sub-critical regimes, $\lambda \leq \lambda_c$, the evolution terminates at a non-equilibrium *jammed* state depending on the initial conditions. In sub-critical regimes, $\lambda < \lambda_c$, the evolution to a final jammed state is exponentially fast in time; in the critical regime, $\lambda = \lambda_c$, the evolution is algebraic. The transition from an equilibrium to a jammed state is a first-order phase transition: The final cluster concentrations C_k undergo a discontinuous jump so that $C_k(\lambda_c + 0) \neq C_k(\lambda_c)$ for $k = 1, 2, \dots$. The first-order character of the phase transition is particularly evident in the case of monomers—their density vanishes for $\lambda \leq \lambda_c$ and remains positive in the super-critical region $\lambda > \lambda_c$.

A peculiar feature of our system is the dependence on the initial conditions. For the case of constant kernels this dependence is a very specific one — only the initial monomer density $c_{1,0}$ and the total density of clusters N_0 are important. For each value of $\lambda > 0$ there exists a domain in the phase plane $(N_0, c_{1,0})$ that corresponds to the super-critical regime where the system evolves to the universal equilibrium state. For the initial conditions outside this domain the system evolution terminates at jammed states. The size of this domain increases with the increasing λ .

For the case of general $0 < s < 1$ the dependence of the evolution regime is more complicated. Although for all $\lambda > 0$ there still exists a domain in the space of initial conditions $\{c_1(0), c_2(0), \dots, c_k(0), \dots\}$, corresponding to the super-critical behavior, the location of this domain is determined by all initial densities $c_k(0)$.

In spite of the simplicity of the model, it reflects some prominent features of the processes of the surface films growth. Hence the possibility of the phase transition in such systems, as well as their dependence on the initial conditions, may be employed for practical manipulations of the surface films properties. It would be also interesting to study similar models in the context of self-assembly, perhaps generalizing the model to allow a few different types of monomers.

[1] M. V. Smoluchowski, Z. Phys. **17**, 557 (1916).
 [2] P. L. Krapivsky, S. Redner, and E. Ben-Naim, *A Kinetic View of Statistical Physics* (Cambridge University Press, 2010).
 [3] F. Leyvraz, Physics Reports **383**, 95 (2003).
 [4] N. V. Brilliantov and P. L. Krapivsky, J. Phys. A **24**,

4787 (1991).
 [5] J. A. Blackman and A. Wieding, EPL **16**, 115 (1991).
 [6] J. A. Blackman and A. Marshall, J. Phys. A **27**, 725 (1994).
 [7] V. Privman, D. V. Goia, J. Park, and E. Matijevic, J. Colloid Interface Sci. **213**, 36 (1999).

- [8] P. Laurençot, *Nonlinearity* **12**, 229 (1999).
- [9] V. Gorshkov and V. Privman, *Physica E* **43**, 1 (2010).
- [10] I. Sevonkaev, V. Privman, and D. Goiaa, *J. Chem. Phys.* **138**, 014703 (2013).
- [11] P. W. K. Rothmund, N. Papadakis, and E. Winfree, *PLoS Biology* **2**, e424 (2004).
- [12] K. Ariga, J. P. Hill, M. V. Lee, A. Vinu, R. Charvet, and S. Acharya, *Sci. Tech. Adv. Mater.* **9**, 014109 (2008).
- [13] V. Privman, *Ann. New York Acad. Sci.* **1161**, 508 (2009).
- [14] A. Demortire, A. Snezhko, M. V. Sapozhnikov, N. Becker, T. Proslie, and I. S. Aranson, *Nature Communications* **5**, 3117 (2014).
- [15] C. G. Evans and E. Winfree, *Chem. Soc. Rev.* **46**, 3808 (2017).
- [16] M. C. Bartelt and J. W. Evans, *Phys. Rev. B* **46**, 12675 (1992).
- [17] H. Kallabis, P. L. Krapivsky, and D. E. Wolf, *EPJB* **5**, 801 (1998).
- [18] A. Pimpinelli and J. Villain, *Physics of Crystal Growth* (Cambridge University Press, 1998).
- [19] M. Zinke-Allmang, *Thin Solid Films* **346**, 1 (1999).
- [20] P. L. Krapivsky, J. F. F. Mendes, and S. Redner, *Phys. Rev. B* **59**, 15950 (1999).
- [21] J. G. Amar, M. N. Popescu, and F. Family, *Phys. Rev. Lett.* **86**, 3092–3096 (2001).
- [22] M. N. Popescu, J. G. Amar, and F. Family, *Phys. Rev. B* **64**, 205404 (2001).
- [23] This may be done in the same manner as for the case of mono-disperse initial conditions: First, we find τ_{\max} from the condition $dc_1(\tau)/d\tau = 0$ at $\tau = \tau_{\max}$, then the condition of interest reads, $c_1(\tau_{\max}) > 0$. It may be recast into the form of Eq. (34)
- [24] The condition $p \rightarrow 0$ corresponds to $\tau \rightarrow \infty$, that is to the super-critical case.